

## Case Study 8

# Monitoring Green Tides in Chinese Marginal Seas

Ming-Xia He<sup>1</sup>, Junpeng Liu<sup>1</sup>, Feng Yu<sup>1</sup>, Daqiu Li<sup>2</sup>, Chuanmin Hu<sup>\*3</sup>

## 8.1 Background

Coastal phytoplankton blooms have been reported world wide. These blooms sometimes cause environmental problems in both developed and developing countries where excessive nutrients and other pollutants from rapid-growing agriculture, aquaculture, and industries are delivered to the ocean. In Chinese coastal waters of the Yellow Sea, East China Sea, and Bohai Sea, the number and size of toxic algae blooms (often called red tides) as well as toxic species have increased significantly since 1998, a result of increased nutrient inputs from multiple sources (Zhou and Zhu, 2006).

Similar to red tides, green tides have also been reported in the world's oceans (e.g., Fletcher, 1996; Blomster et al, 2002; Nelson et al. 2003; Merceron et al., 2007). These green tides contain high concentrations of green macroalgae, but they are typically small in size and restricted to coastal areas. However, between May and July 2008, an extensive bloom of the green macroalgae *Ulva prolifera* (previously known as *Enteromorpha prolifera*, see Hayden et al., 2003) occurred in coastal and offshore waters in the Yellow Sea (YS) near Qingdao, China (Hu and He, 2008). The macroalgae bloom created an enormous burden on local government and management agencies because all the algae that washed up onto the beach and in the Olympic sailing area near Qingdao had to be physically removed (Figure 8.1). By the end of July 2008, >1,000,000 tons of algae had been removed. Other methods (e.g., using a 30-km boom) were employed to maintain an algae-free area of water near Qingdao for the Olympic sailing competition, with a total cost exceeding US\$100 million (Wang et al., 2009; Hu et al., 2010). The bloom was first speculated to be a result of local pollution, but analysis of MODIS (Moderate Resolution Imaging Spectroradiometer) satellite imagery revealed a remote origin (Hu and He, 2008). More recent studies suggested that the bloom was a result of rapid expansion of the coastal seaweed aquaculture

<sup>1</sup>Ocean Remote Sensing Institute, Ocean University of China, 5 Yushan Road, Qingdao, China 266003

<sup>2</sup>Institute for Environmental Protection Science at Jinan, 183, Shanda Road, Jinan, China 250014

<sup>3</sup>College of Marine Science, University of South Florida, 140 7th Ave., S., St. Petersburg, FL 33701, USA. \*Email address: [hu@marine.usf.edu](mailto:hu@marine.usf.edu)

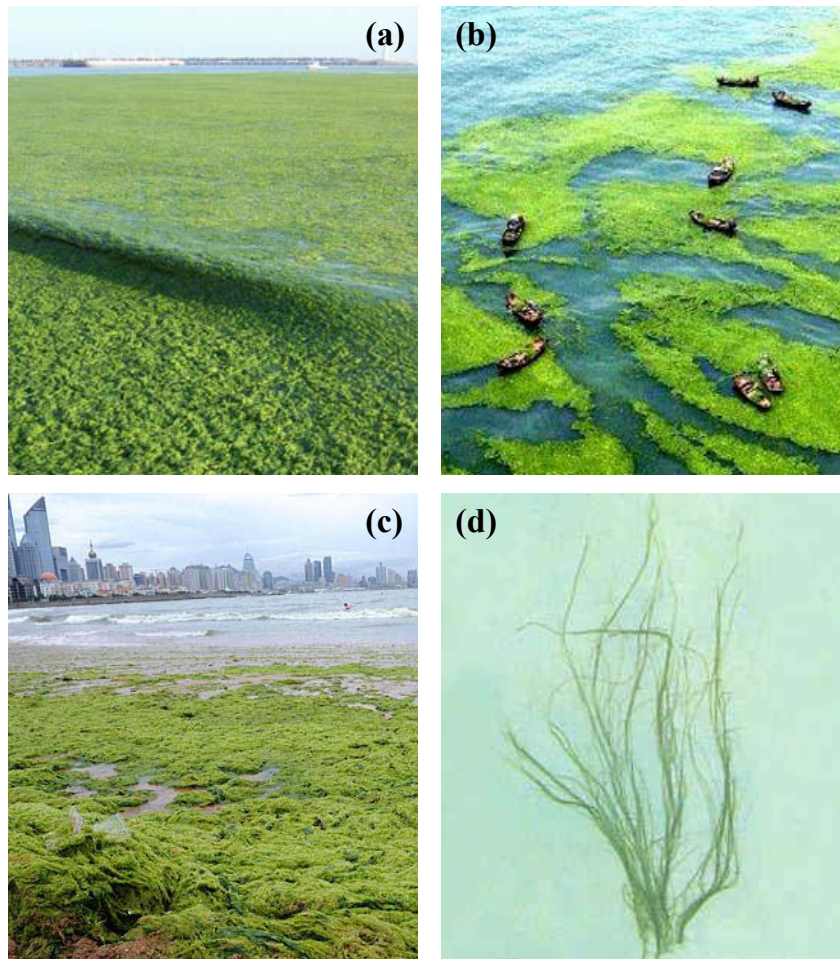


**Figure 8.1** Green tide of macroalgae *Ulva prolifera* in coastal waters of the Yellow Sea near Qingdao, China. (a) and (b) Macroalgae blooms in coastal waters; (c) algae washed onto the beach; (d) morphology of the algae, which can grow to >1 m in length. (Images from public news media [http://tupian.hudong.com/a2\\_70\\_76\\_01300000195282124057760319832\\_jpg.html](http://tupian.hudong.com/a2_70_76_01300000195282124057760319832_jpg.html)).

of *P. yezoensis* where water circulation and favourable growth conditions brought remote *U. prolifera* to Qingdao (Li et al., 2008; Liang et al., 2008; Lü and Qiao, 2008; Qiao et al., 2008; Sun et al., 2008; Hu, 2009; Liu et al., 2009; Hu et al., 2010). Further, it was found that smaller green macroalgae blooms were recurrent in history not only in the Yellow Sea but also in the East China Sea (ECS) (Hu et al., 2010). Because green tides of the same macroalgae may occur in the future in both YS and ECS, it is desirable to establish a remote-sensing based monitoring system to provide timely information on the occurrence and characteristics of green tides (location, size, and potential trajectory). Indeed, a rapid-response remote sensing system using multiple satellites was critical in helping to implement management plans during the 2008 bloom event (Jiang et al., 2009). Here, using data from several

satellite instruments, we describe the methodology used to detect green tides, and a preliminary monitoring system that covers the entire YS and ECS (Figure 8.2). Our primary objective is to demonstrate the methods used to identify green tides from space, which may be applied in other coastal regions where similar green tides also occur.

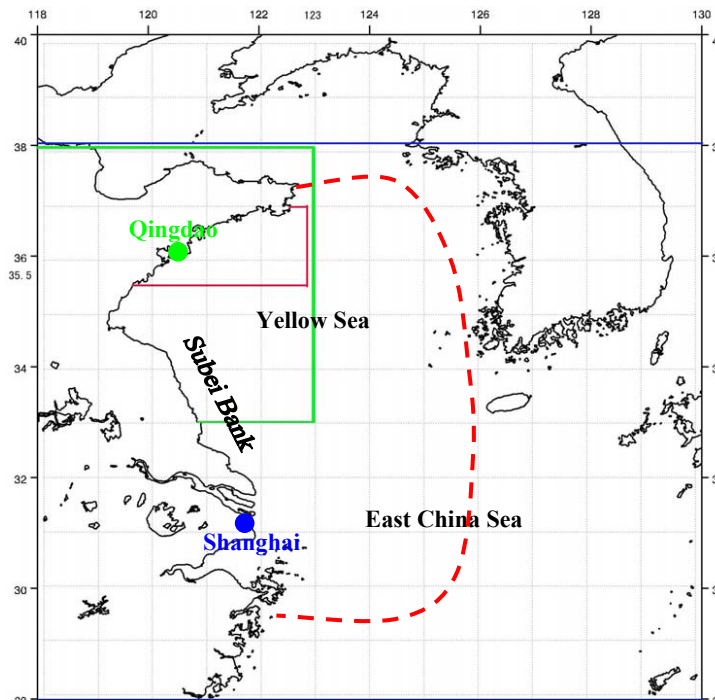


**Figure 8.2** Geographic areas (dashed red line) where green tides of the macroalga *Ulva prolifera* were found between 2000 and 2009. Our monitoring efforts are focused on the Yellow Sea and East China Sea. The various colour boxes represent several pre-defined regions to facilitate image display and interpretation. An experimental online monitoring system has been established and has been in operation since early 2009: <http://www.station.orsi.ouc.edu.cn:8080/algae/>.

## 8.2 Data and Methods

Three types of data were used. Type 1 is near real-time data obtained from the MODIS instruments onboard the U.S. NASA satellites Terra (1999 – present) and Aqua (2002 – present), and the MERSI (Medium Resolution Spectral Imager) instrument onboard the Chinese satellite FY-3A (2008 – present). These satellite instruments have a wide swath width (>2000 km) and frequent coverage, and provide medium-resolution (250-m) data suitable for identifying large-scale macroalgae blooms. Although the individual multi-cell algae are thin and small (Figure 8.1), their aggregation makes

them appear as surface vegetation and therefore detectable in satellite imagery. Type 2 is high-resolution data from satellite instruments designed for land and coastal waters, for example Landsat, SPOT, Synthetic Aperture Radar (SAR), and HJ-1. These data have limited spatial (hundreds of kilometers) and infrequent (one week to 16 days) coverage, but can be used to detect small-scale macroalgae blooms. Type 3 is near-real time data from MODIS, MERSI, COCTS (onboard the Chinese satellite HY-1B, 2007 – present), and QuikScat (1999 – present). These data can provide environmental conditions of the study regions, including sea surface temperature (SST), sea surface wind (SSW), and ocean chlorophyll-*a* concentrations.

For brevity, in this work we demonstrate primarily how to use MODIS (Type 1 data) and Landsat (Type 2 data) to detect macroalgae blooms in open oceans and coastal waters. The use of Type 3 data to assess environmental conditions is shown in other case studies. MODIS data source and most processing methods are described in detail in Case Study 2 (*Detection of Oil Slicks using MODIS and SAR Imagery*), but for completeness they are summarized here. All data were downloaded from the U.S. NASA Goddard Space Flight Center (GSFC) at no cost (<http://oceancolor.gsfc.nasa.gov>). The data are open to the public in near real-time and do not require data subscription. The following steps were used to generate geo-referenced MODIS products at 250-m resolution.

**Step 1:** MODIS Level-0, 5-minute granules (satellite data collected every 5 minutes were stored in a computer file to facilitate data management) were downloaded from NASA/GSFC;

**Step 2:** MODIS Level-0 data were processed to generate Level-1b (calibrated total radiance) data for the 36 spectral bands using the SeaWiFS Data Analysis System (SeaDAS) software. The software was originally designed to process SeaWiFS data only, but was updated to process data from other satellite instruments including MODIS. The free software is distributed by the U.S. NASA GSFC. The Level-1b data were stored in computer files in Hierarchical Data Format (HDF);

**Step 3:** MODIS Level-1b data were used to derive the spectral reflectance:

$$R_{rc,\lambda}(\theta_0, \theta, \Delta\phi) = \pi L_{t,\lambda}^*(\theta_0, \theta, \Delta\phi) / (F_{0,\lambda} \times \cos\theta_0) - R_{r,\lambda}(\theta_0, \theta, \Delta\phi), \quad (8.1)$$

where  $\lambda$  is the wavelength for the MODIS band,  $L_t^*$  is the calibrated sensor radiance after correction for gaseous absorption,  $F_0$  is the extraterrestrial solar irradiance,  $(\theta_0, \theta, \Delta\phi)$  represent the pixel-dependent solar-viewing geometry, and  $R_r$  is the reflectance due to Rayleigh (molecular) scattering. This step used the software CREFL from the NASA MODIS Rapid Response Team. The  $R_{rc}$  data of the 7 MODIS bands (469, 555, 645, 859, 1240, 1640, and 2130 nm) were stored in HDF computer files.

**Step 4:** The  $R_{rc}$  data were geo-referenced to a rectangular (also called geographic lat lon) projection for the area of interest, defined by the North-South and East-

West bounds. Because 1 degree is about 110 km at the equator, the map-projected data have 440 image pixels per degree, corresponding to 250 m per image pixel. Although only the MODIS 645- and 859-nm bands have a nadir resolution of 250 m, other bands at 500-m resolution were interpolated to 250-m resolution using a sharpening scheme similar to that for Landsat (i.e., the 250-m data at 645 nm were congregated to 500-m data, and the ratios between a congregated 500-m pixel and the 4 individual 250-m pixels were applied to "sharpen" the MODIS 500-m data from other bands). The mapping software was written in-house using C++ and PDL (Perl Data Language) with a mapping accuracy of about 0.5 image pixel;

**Step 5:** The map projected  $R_{rc}$  data at 645, 555, and 469 nm were converted to byte values using a logarithmic stretch, and then used as the Red, Green, and Blue channels, respectively, to compose a RGB image. The purpose was to visually identify land and clouds;

**Step 6:** A floating algae index (FAI) data product was derived as follows (Hu, 2009):

$$FAI = R_{rc,NIR} - R_{rc,NIR'},$$

$$R_{rc,NIR'} = R_{rc,RED} + (R_{rc,SWIR} - R_{rc,RED}) \times (\lambda_{NIR} - \lambda_{RED}) / (\lambda_{SWIR} - \lambda_{RED}), \quad (8.2)$$

where  $R_{rc,NIR'}$  is the baseline reflectance in the NIR band derived from a linear interpolation between the RED and shortwave IR (SWIR) bands. For MODIS,  $\lambda_{RED} = 645$  nm,  $\lambda_{NIR} = 859$  nm,  $\lambda_{SWIR} = 1240$  nm. FAI was designed to quantify the reflectance in the near-IR due to the vegetation "red-edge" effect, because green macroalgae floating on the water surface appear as surface vegetation;

**Step 7:** The RGB and FAI images were loaded in the software ENVI for display and analysis. The "Link Display" function connects the two image types, so a suspicious macroalgae slick/patch in the FAI image can be cross-examined with the RGB image to determine if it might be caused by small clouds instead of macroalgae.

Landsat-5 TM and Landsat-7 ETM+ Level-1b data were obtained from the U.S. Geological Survey at no cost (<http://glovis.usgs.gov>). These are radiometrically calibrated radiance data in seven spectral channels, geo-referenced to a UTM projection and stored in Geo-TIFF computer files. The same steps used for MODIS were used to generate Landsat RGB and FAI images using computer codes developed in-house, except that Landsat wavebands of  $\lambda_{RED} = 660$  nm,  $\lambda_{NIR} = 825$  nm, and  $\lambda_{SWIR} = 1650$  nm were used in Equation 8.2 to derive a Landsat FAI.

### 8.3 Demonstration

Figure 8.3 shows a MODIS 250-m resolution FAI image covering a portion of the YS, where land and clouds are masked by the RGB image, obtained on 29 June 2008. Two extensive bloom areas are outlined in the dashed circles. These are blooms of the



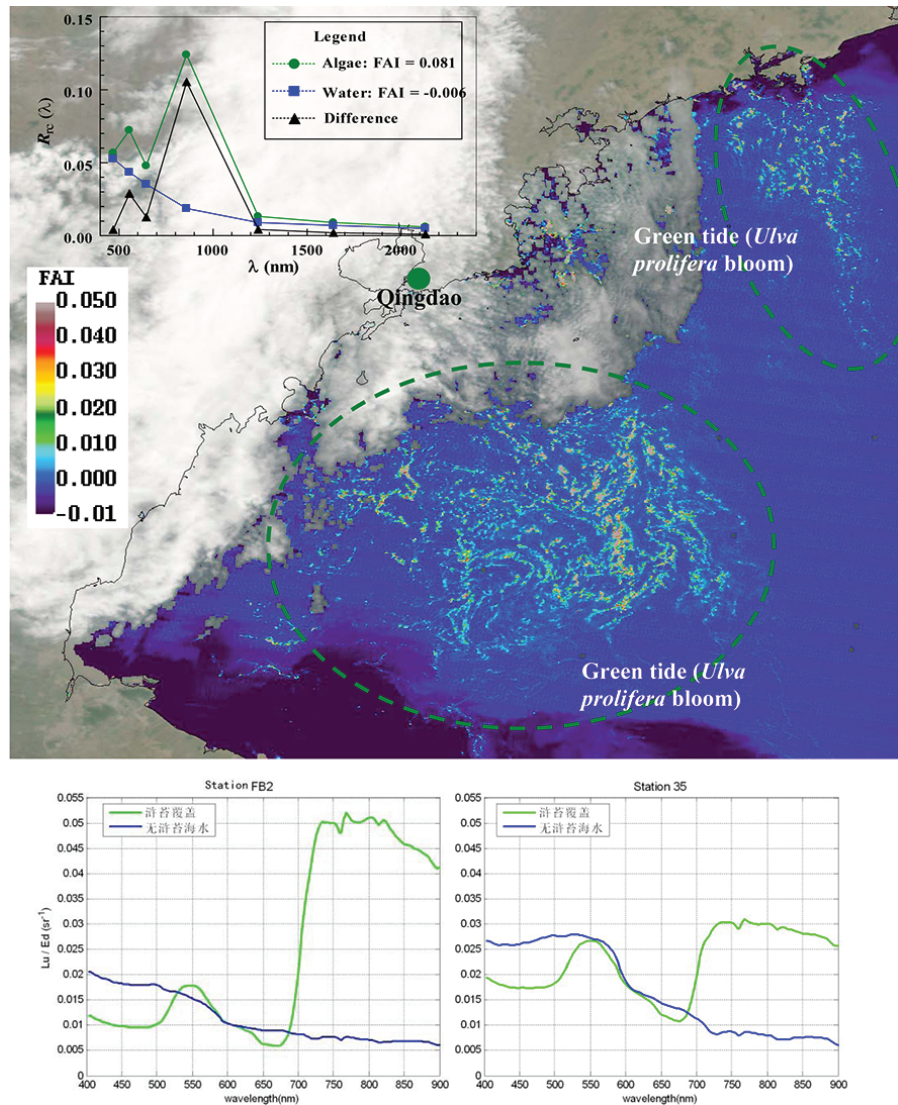


**Figure 8.3** Top: MODIS floating algae index (FAI) image on 29 June 2008 showing green tides (*Ulva prolifera* blooms) in the Yellow Sea near Qingdao, China. The image covers the area of 34.5°N - 37°N and 119°E - 122°E. Cloud and land masks are overlaid on the image. The reflectance spectra of an identified algae pixel and a water pixel are shown in the inset figure. Bottom: Reflectance spectra measured from macroalgae mats (green lines) and algae-free water (blue lines) in the same region, from two different stations.

green macroalgae, *U. prolifera*, as confirmed by concurrent management activities (>1000 vessels were utilized to clean the algae in this region between late June and early August 2008, with >1,000,000 tons of algae collected). Examination of the  $R_{TC,\lambda}$  spectral shapes of individual pixels from the slicks/patches show enhanced reflectance in the NIR, typical for surface vegetation. An example is shown in the

inset figure of Figure 8.3, where the spectral shape from the algae pixel is very similar to those obtained from *in situ* measurements from *U. prolifera* surface mats in the same region (Figure 8.3 bottom panels). Even though the *in situ* reflectance is defined differently (i.e., with units of  $\text{sr}^{-1}$ ) and MODIS  $R_{\text{rc},\lambda}$  is not corrected for aerosol scattering effects, they both show elevated reflectance in the NIR and in the green (555 nm).

Not every MODIS 250-m pixel is covered completely by the algae. Rather, the pixels may be mixed with algae and water. The linear design of FAI (Equation 8.2) makes the unmixing straightforward. Assuming  $\text{FAI} \leq 0.0$  for 0% algae coverage in a pixel and  $\text{FAI} \geq 0.02$  for 100% coverage in a pixel (these threshold values were determined by image gradient analysis and visual interpretation), algae coverage for FAI values between 0.0 and 0.02 can be determined using a linear interpolation. For the image shown in Figure 8.3, the total number of MODIS 250-m pixels containing the macroalgae was estimated to be 70,333, corresponding to an area of about 3600  $\text{km}^2$ . After linear unmixing, the coverage area of algae was estimated to be 1101  $\text{km}^2$ . The coverage area estimate, however, has some degree of uncertainty and requires field validation.

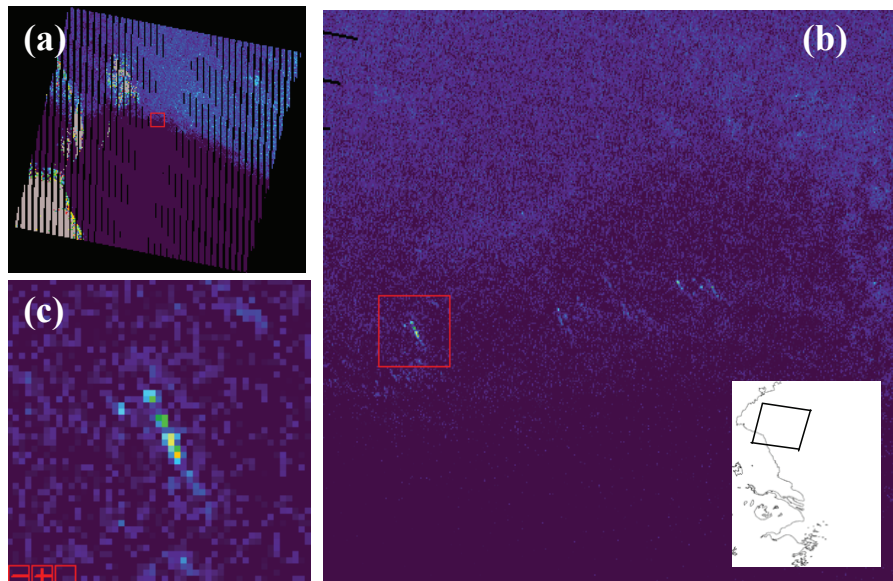


**Figure 8.4** (a) Landsat-7 ETM+ FAI image on 10 May 2008 covering the northern portion of Subei Bank, where the purple colour indicates high sediment concentrations. (b) A sub-scene of 512 x 512 pixels as outlined by the red box in (a). Inset figure shows the location of the Landsat image. (c) An enlarged portion of (b) showing the algae slick.

For the MODIS instrument sensitivity, we determined that the smallest size of the algae slick that MODIS FAI imagery could reveal was about 5 m, if the slick was at least 3 – 4 pixels in length (Hu et al., 2010). Smaller algae, especially during bloom initiation, could not be detected by MODIS, but could be detected by higher-

resolution instruments such as Landsat TM and ETM+. Figure 8.4 shows a sub-scene of a Landsat ETM+ FAI image collected on 10 May 2008 in the north of the Subei Bank. The small slicks of algae are impossible to find in the corresponding MODIS FAI image, but the spectral shapes show elevated reflectance in the NIR, indicating macroalgae blooms. Indeed, Landsat and MODIS were combined to reveal the temporal evolution of the 2008 bloom event, with the conclusion that the bloom started in near-shore waters of the shallow Subei Bank (Hu et al., 2010) where aquaculture of the seaweed *P. yezoensis* was practiced every year.

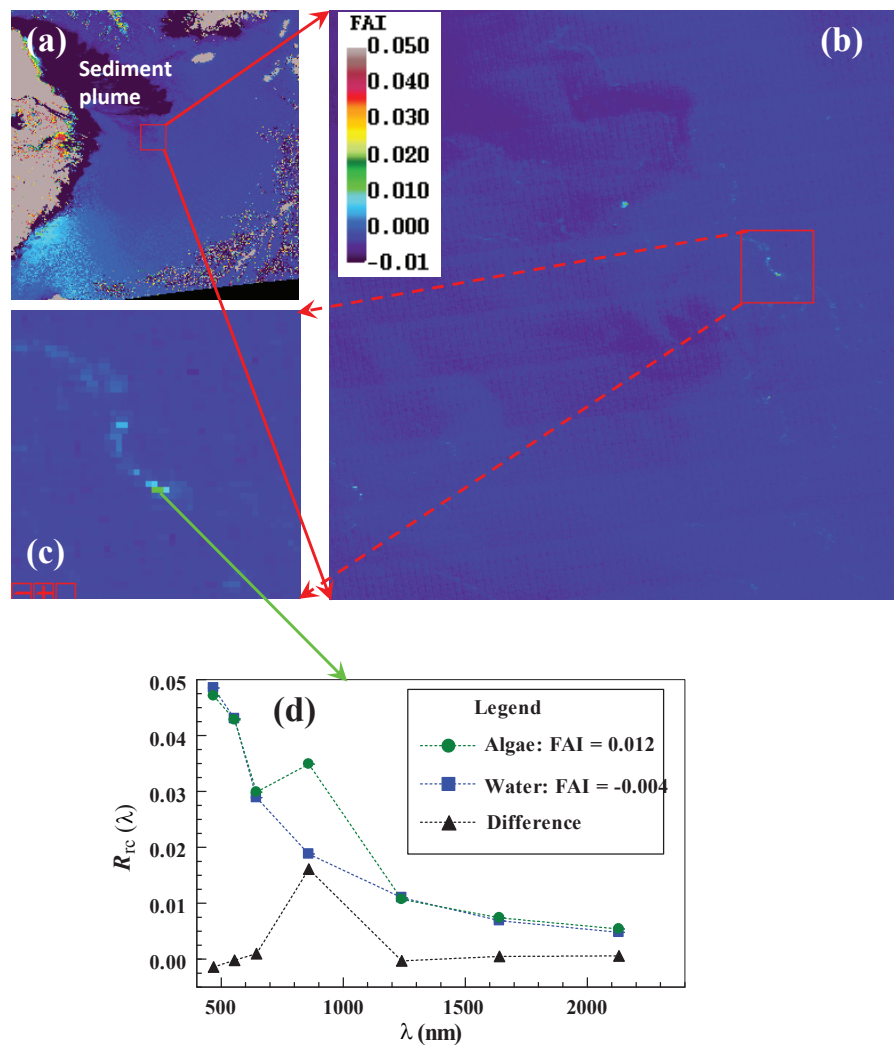


**Figure 8.5** (a) MODIS-Aqua 250-m resolution FAI image on 28 April 2009 covering the ECS. (b) A sub-scene of about 100 x 100 km east of the Changjiang River mouth. (c) An enlarged portion of (b) showing the algae slick. (d) The reflectance spectra of the identified algae pixel and nearby water pixel.

The retrospective analysis of satellite imagery showed the origin, size, distribu-



tion, and evolution of the 2008 bloom event as well as smaller blooms in previous years (Hu et al., 2010). For the purpose of monitoring, MODIS data were obtained and analyzed in near real-time since early 2009 to monitor the bloom conditions in both YS and ECS (Figure 8.2). The earliest MODIS FAI image where algae slicks can be identified, obtained on 28 April 2009 from the Aqua satellite, is shown in Figure 8.5. The MODIS image shows some slicks about 200 km east of the Changjiang River mouth in the downstream of a NW – SE sediment plume from the Subei Bank, indicating that the algae slicks originated from nearshore waters of the Subei Bank. This is the same place where the 2008 macroalgae bloom originated. Spectral shapes of the algae pixels show elevated reflectance in the NIR (Figure 8.5d), suggesting that this is some kind of floating vegetation. Considering the proximity to the coast and the same origin as for the 2008 bloom, it is very likely that the algae is the same type, i.e., *U. prolifera* from expanded seaweed aquaculture. Note that this analysis is based on MODIS data alone. Information derived from circulation models and environmental conditions (e.g., wind) provides additional evidence that these algae slicks can be *U. prolifera* (Hu et al., 2010).

## 8.4 Training

MODIS reflectance data collected on 19 May 2009 and 14 June 2000, and their corresponding RGB and FAI images for the ECS can be downloaded from the IOCCG website (<http://www.ioccg.org/handbook/He/>) for the demonstration on how to identify algae slicks and other features. Because of the synoptic coverage (often >10 degrees in both N-S and E-W directions) and medium resolution (250-m per pixel), the MODIS images are very large. Thus, commercial software packages (e.g., ENVI, ArcInfo, Erdas Imagine, or any other software that has basic image processing capabilities) are required to focus on a particular region. Here we use the software ENVI to demonstrate how to identify the algae slicks using the following visualization and analysis.

First, the RGB image is loaded into ENVI by using the "File -> Open Image File" function. Three display windows are shown (similar to Figures 8.6 a-c): scroll, image, and zoom. The scroll window shows the entire region at reduced resolution to serve as a browse image; the image window shows a portion of the image at full resolution (250-m); and the zoom image enlarges a smaller portion by 4 times. During the initial display in ENVI, the colours are stretched using histogram balancing over the entire image. The image window can be colour enhanced by a "Gaussian" or linear enhancement, using the menu of "Image -> Enhance".

Next, the FAI image is loaded into ENVI in the same way. The "Link Display" function is used to link the two images so that they can be cross examined. This way, any suspicious features identified on the FAI image can be easily determined if they are from clouds or land.

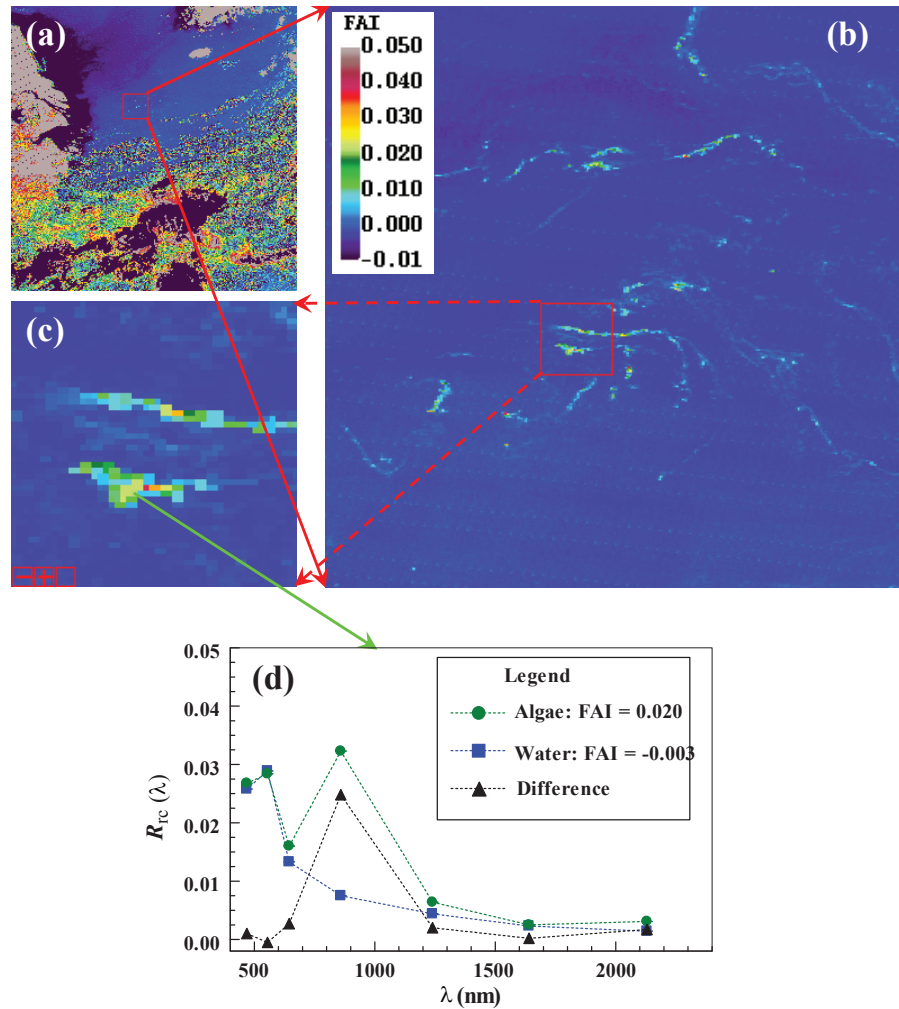


**Figure 8.6** (a) MODIS-Terra 250-m FAI image on 19 May 2009 covering the ECS. (b) A sub-scene of about 100 x 100 km east of the Changjiang River mouth is shown at 250-m resolution. (c) An enlarged portion of (b) showing the algae slick. (d) The reflectance spectra of the identified algae pixel and nearby water pixel.

Finally, the image window in the scroll image is moved to examine the entire image step by step. It is easy to find that clouds and land show high FAI values. In cloud-free waters, there are also some slicks associated with high FAI values, as shown in Figure 8.6b. The same steps are applied to display the MODIS FAI image from 14 June 2000 (Figure 8.7).

## 8.5 Questions

**Q1:** Are the high-FAI slicks in Figure 8.6b the green macroalgae *Ulva prolifera*?

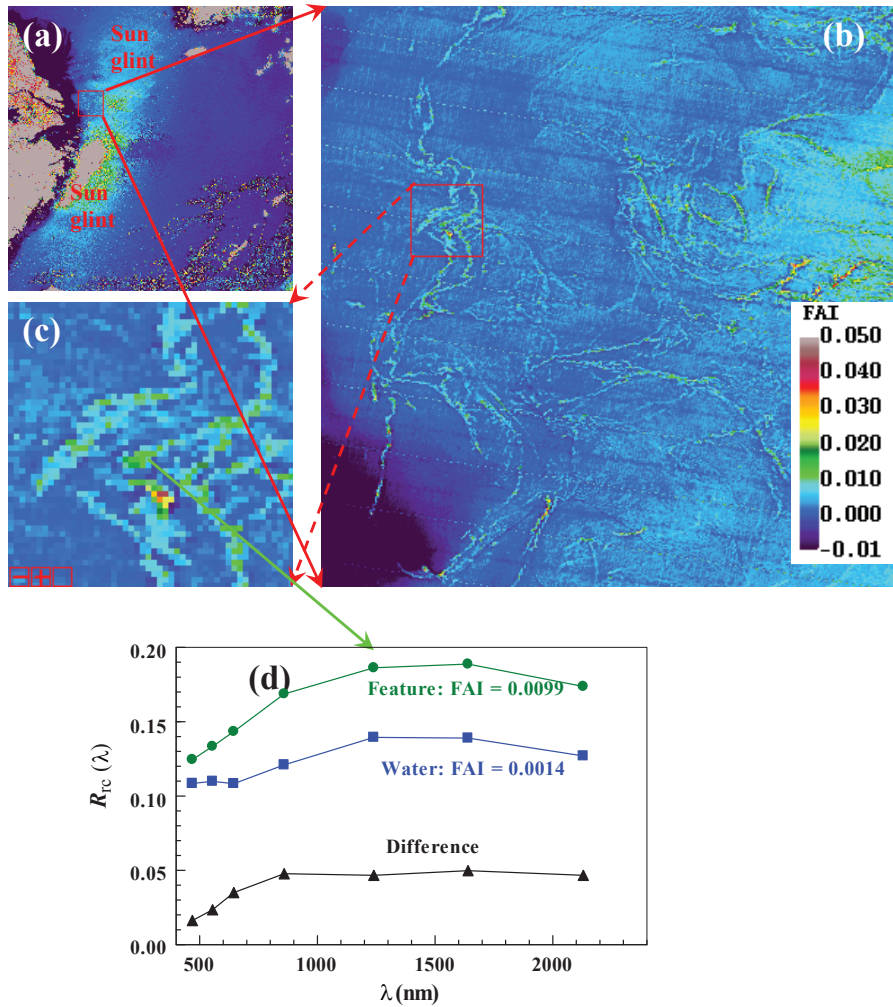


**Figure 8.7** (a) MODIS-Terra 250-m FAI image on 14 June 2000 covering the ECS. (b) A sub-scene of about 100 x 100 km east of the Changjiang River mouth is shown at 250-m resolution. (c) An enlarged portion of (b) showing some suspicious slicks. (d) The reflectance spectra of the suspicious feature and a nearby water pixel. Their difference spectrum is also shown.

**Q2:** Are the high-FAI slicks in Figure 8.7b the green macroalgae *Ulva prolifera*?

## 8.6 Answers

**A1:** Very likely. Once clouds and sun glint can be ruled out as the potential cause of the slicks, it is almost certain that they are some sort of surface vegetation. However, to add more confidence, reflectance spectra of the identified slicks and the nearby water can be examined. Similar to the case for Figure 8.5,  $R_{rc,\lambda}$  spectra extracted from pixels of the suspicious slicks show elevated reflectance in the NIR, where an

example is presented in Figure 8.6d. The data are extracted from the HDF data file for the locations (in image pixel line coordinates) of the slicks and nearby waters. The data extraction can be achieved through ENVI or simple computer programs. Although the high NIR reflectance is only an indication of surface vegetation and not necessarily the green macroalgae *Ulva prolifera*, the same arguments applied to Figure 8.5 can be used here to infer the algae type. In particular, the location is almost the same as three weeks ago (Figure 8.5) but the size is much larger, suggesting algae growth in this offshore region.

**A2:** Although the slicks appear to be floating algae, it is difficult to determine from the FAI image alone whether the suspicious features are freshwater slicks or whether they are due to water convergence, because the region is contaminated by significant sun glint (the extensive NE - SW high FAI band in Figure 8.7a).  $R_{rc,\lambda}$  spectra extracted from pixels of the suspicious features show elevated reflectance in all wavelengths (Figure 8.7d), and their difference from the nearby water spectra do not show distinctive peaks at 859 nm, but rather show flat spectra from 859 to 2130 nm. Therefore, it is unlikely that these high-FAI slicks are floating algae. Indeed, cloud-free and glint-free images from adjacent days do not show similar slicks in the same region, confirming this speculation. However, the origin of the slicks, whether from freshwater or from water convergence, is still unclear.

## 8.7 Discussion and Summary

Visualization of suspicious slicks in MODIS 250-m imagery and Landsat 30-m imagery is relatively easy. Indeed, an interactive colour stretch applied in ENVI to the single 859-nm band, as referenced against the corresponding RGB image (to detect clouds), can also reveal the same algae slicks. However, this is labour intensive due to the interactive colour stretch. First, it is difficult to establish a consistent time-series because the single band still contains variable aerosol contributions. Likewise, although a simple Normalized Difference Vegetation Index (NDVI) based on the  $R_{rc,\lambda}$  data partially removes the influence of aerosols and varying solar/viewing geometry, the residual uncertainties due to these spatially and temporarily varying properties can lead to highly variable NDVI values for the same targets. In contrast, the baseline subtraction method used in FAI serves as a simple but effective atmospheric correction, where FAI values from the same algae and water pixels remain relatively stable under varying conditions (Hu, 2009). The linear design also makes unmixing of mixed algae-water pixels straightforward. Thus, FAI is preferred to detect and quantify macroalgae blooms.

In this exercise, one must be cautious of the interpretation of suspicious slicks identified visually, especially in sun glint regions. Analysis of the spectral shape of the suspicious features and visual examination of images collected from adjacent days can add more confidence. The most difficult scenario is cloud masking. Clouds



are visually determined through examining RGB images. The reason for this is that although several cloud masking algorithms have been proposed and used to process MODIS data, in the YS and ECS where aerosols can sometimes lead to  $R_{rc,NIR}$  and  $R_{rc,SWIR}$  significantly higher than the pre-defined threshold reflectance for clouds, the cloud masks may reduce data coverage. Relaxing such threshold values, on the other hand, may lead to cloud pixels undetected. Developing a reliable cloud-detection algorithm specifically for this region should be the next step in this effort.

Synthetic Aperture Radar (SAR) can penetrate clouds. Limited SAR data suggest that green tide macroalgae blooms appear as bright slicks in C-band images but dark slicks in L-band images. SAR data therefore serve as an additional data source for green tide monitoring, although they have less spatial/temporal coverage and are not free. Likewise, data from other medium-resolution instruments (e.g., MERSI is equipped with similar 250-m bands as MODIS) and high-resolution instruments (e.g., HJ-1 is equipped with similar 30-m bands as Landsat TM and ETM+) can also provide complementary information to enhance our capability in green tide monitoring.

This work is focused on the green tide detection method. Understanding of the green tide characteristics (occurrence frequency, initiation, evolution, physiology, ecology, etc.), on the other hand, requires coordinated inter-disciplinary efforts in studying phytoplankton ecology, ocean circulation, and environmental forcing for algae growth (nutrient availability, temperature, etc.). These are beyond the scope of the current demonstration, but can be found in the refereed literature (e.g., Taylor et al., 2001; Merceron et al., 2007; Yuan et al., 2008). Our monitoring efforts, however, do include routine generation and analysis of ocean SST, wind, and chlorophyll-*a* concentrations. These properties provide ancillary information to understand the environmental conditions of the observed macroalgae blooms in the YS and ECS.

In summary, data from a suite of satellite instruments, from the medium-resolution MODIS and MERSI to the high-resolution Landsat and HJ as well as the cloud-free SAR, are effective in detecting blooms of the green macroalgae *Ulva prolifera* (green tides) in the YS and ECS under various conditions. Combined with other ancillary information, these data form the basis to establish a semi-operational monitoring system, currently being developed and operated jointly at the Ocean Remote Sensing Institute of the Ocean University of China (<http://www.station.orsi.ouc.edu.cn:8080/algae/>) and the Optical Oceanography Lab of the University of South Florida. This case study presents an example of how satellite imagery can be used to help understand and manage our coastal environments. Similar systems may be established for other coastal regions where green tides also occur.

### 8.7.1 Acknowledgements

This work was supported by the U.S. NASA (NNX09AE17G) and NOAA (NA06NES4400004), by a special project of the Qingdao government (NO.09-2-5-4-HY), and by the EU

FP6 DRAGONESS Project (No. SSA5.CT.2006- 030902) and the ESA-MOST Dragon Programme Ocean Project (ID2566). We thank the US NASA/GSFC and USGS for providing MODIS and Landsat data.

## 8.8 References

- Blomster J, Back S, Fewer DP, Kiirikki M, Lehvo A, Maggs CA, Stanhope MJ (2002) Novel morphology in *Enteromorpha* (Ulvophyceae) forming green tides. *Am J Bot* 89:1756-1763
- Fletcher, RL (1996) The occurrence of "green tides": a review In: Schramm W, Nienhuis PH ( eds) *Marine benthic Vegetation: recent changes and the effects of eutrophication*. Springer, Berlin, Germany, p 7-43
- Hayden HS, Blomster J, Maggs CA, Silva PC, Stanhope MJ, Waaland JR (2003) Linnaeus was right all along: *Ulva* and *Enteromorpha* are not distinct genera. *European J Phycol* 38:277-294
- Hu C, He M-X (2008) Origin and offshore extent of floating algae in Olympic sailing area. *EOS AGU Trans* 89(33): 302-303
- Hu C (2009) A novel ocean color index to detect floating algae in the global oceans. *Remote Sens Environ* 113: 2118-2129
- Hu C, Li D, Chen C, Ge J, Muller-Karger FE, Liu J, Yu F, He M-X (2010) On the recurrent *Ulva prolifera* blooms in the Yellow Sea and East China Sea. *J Geophys Res* 115: C04002, doi:10.1029/2009JC005511
- Jiang X, Liu J, Zou B, Wang Q, Zeng T, Guo M, Zhu H, Zou Y, Tang J (2009) The satellite remote sensing system used in emergency response monitoring for *Enteromorpha prolifera* disaster and its application. *Acta Oceanol Sin* 31: 52-64
- Li D, He S, Yang Q, Lin J, Yu F, He M-X, Hu C (2008) Origin and distribution characteristics of *Enteromorpha prolifera* in sea waters off Qingdao, China. *Environ Protection* 402(8B): 45-46 (in Chinese)
- Liang Z, Lin X, Ma M, Zhang J, Yan X, Liu T (2008) A preliminary study of the *Enteromorpha prolifera* drift gathering causing the green tide phenomenon. *Periodical of Ocean University of China* 38(4): 601-604 (in Chinese, with English abstract)
- Liu D, Keesing JK, Xing Q, Shi P (2009) World's largest macroalgal bloom caused by expansion of seaweed aquaculture in China. *Mar Sci Bulletin* doi:101016/jmarpolbul200901013
- Lü X, Qiao F (2008) Distribution of sunken macroalgae against the background of tidal circulation in the coastal waters of Qingdao, China, in summer 2008. *Geophys Res Lett* 35: L23614, doi:101029/2008GL036084
- Merceron M, Antoine V, Aubry I, Morand P (2007) *In situ* growth potential of the subtidal part of green tide forming *Ulva* spp. stocks. *Sci Tot Environ* 384: 293-305
- Nelson TA, Nelson AV, Tjoelker M (2003) Seasonal and spatial patterns of "Green tides" (Ulvoid algal blooms) and related water quality parameters in the coastal waters of Washington state, USA. *Botanica Marina* 46: 263-275
- Qiao F, Ma D, Zhu M, Li MR, Zang J, Yu H (2008) Characteristics and scientific response of the 2008 *Enteromorpha prolifera* bloom in the Yellow Sea. *Adv Mar Sci* 26(3): 409-410 (in Chinese)
- Sun S, Wang F, Li C, Qin S, Zhou M, Ding L et al (2008) Emerging challenges: Massive green algae blooms in the Yellow Sea. *Nature Precedings*, hdl:10101/npre200822661
- Taylor R, Fletcher RL, Raven JA (2001) Preliminary studies on the growth of selected green-tide algae in laboratory culture: effects of irradiance, temperature, salinity and nutrients on growth rate. *Botanica Marina* 44: 327-336
- Wang J, Yan B, Lin A, Hu J, Shen S (2007) Ecological factor research on the growth and induction of spores release in *Enteromorpha Prolifera* (Chlorophyta). *Mar Sci Bull* 26 (2): 60-65
- Yuan D, Zhu J, Li C, Hu D (2008) Cross-shelf circulation in the Yellow and East China Seas indicated by MODIS satellite observations. *J Marine Sys* 70:134-149
- Zhou, MJ, Zhu MY (2006) Progress of the Project "Ecology and Oceanography of Harmful Algal Blooms in China". *Adv Earth Sci* 21: 673-679